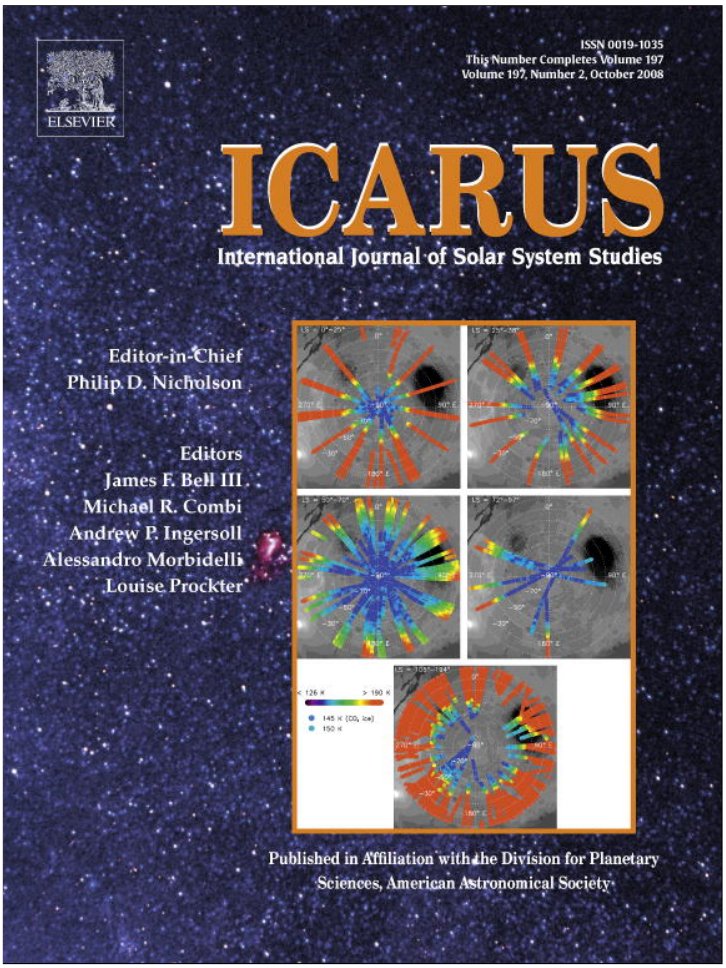

Icarus 197 (2008) 452–457

Contents lists available at ScienceDirect

Icarus

www.elsevier.com/locate/icarus

On the origin of a double, oblique impact on Mars

J.E. Chappelow [a,b,*], R.R. Herrick [b]

[a] Arctic Region Supercomputing Center, University of Alaska Fairbanks, PO Box 756020, Fairbanks, AK 99775-6020, USA
[b] Geophysical Institute, University of Alaska Fairbanks, PO Box 757320, Fairbanks, AK 99775-7320, USA

ARTICLE INFO

Article history:
Received 30 January 2008
Revised 14 April 2008
Available online 19 June 2008

Keywords:
Mars
Mars, satellites
Impact processes

ABSTRACT

A double, oblique impact feature north of Olympus Mons provides a unique opportunity to investigate the event that formed it. The sizes of the craters, their ellipticity, shapes of ejecta blankets, separation from each other, and positions relative to each other, all give us information about the event. Coupling this information with an existing model of meteoritic flight through an atmosphere allows us to test several possible scenarios for the event (object type and origin, pre-entry trajectory, atmospheric trajectory, prevailing atmospheric density). We find it highly improbable that the impactor was simply an extra-martian asteroid or comet. We also find that it is unlikely to have been a double-asteroid or a tidally fractured one, but is more likely to have been a Mars-orbiting moonlet whose orbit tidally decayed, and that denser atmospheric conditions than today's may have prevailed when it impacted.

1. Introduction

Based on counts of martian elliptical craters, Schultz and Lutz-Garihan (1982) and Bottke et al. (2000) came to differing conclusions regarding the craters' origins. Using an estimate for the threshhold impact angle below which impact craters become elliptical (θ_{thresh}) of 5° (from Gault and Wedekind, 1978), and an assumed $\sin^2\theta$ impact angle cumulative probability distribution, Schultz and Lutz-Garihan (1982) inferred that Mars holds an excess of high-obliquity impact craters. They concluded that many of these craters represent the impacts of a former population of martian moonlets whose orbits tidally decayed. Phobos, which will also impact Mars in a few million years when its orbit tidally decays, and Deimos which will not (e.g. Lambeck, 1979), were proposed to be remnant members of this population. However, using a higher value of θ_{thresh} (12°) that they derived, Bottke et al. (2000) concluded that no such excess of elliptical craters exists, compared to the Moon and Venus, and that all or most of these craters were formed by simple extra-martian asteroid impacts.

One feature identified by Gault and Wedekind (1978), and included in both Schultz and Lutz-Garihan (1982) and Bottke et al. (2000), presents a unique opportunity to investigate the properties and trajectory of the impactor that formed it, and to attempt to determine what sort of event formed it. The feature is a double, elliptical impact feature located on a flat, level plain just north of Acheron Fossae, at 40.5° N, 222.5° E (Fig. 1), within a unit identified as HTa on the map by Tanaka et al. (2005). Via crater counting, Tanaka et al. dated this unit at late Hesperian in age; the double crater excavated from it is therefore late Hesperian or younger in age, and probably formed long after Mars lost any postulated early, dense atmosphere (e.g. Jakosky and Phillips, 2001; Craddock and Howard, 2002). 'Blowouts' on the eastern ends of each crater, and the form of the western 'forbidden zone' in the larger crater's ejecta demonstrate that the impactors were traveling almost due west-to-east (and therefore in the prograde direction of Mars's rotation) at the time of impact. The smaller crater (2.0 km × 3.0 km) lies ~12.5 km almost directly up-range of the larger one (7.5 km × 10.0 km). This alignment of the craters strongly suggests that they were formed by two pieces of a larger object which fractured high in the atmosphere, and were then separated by differential atmospheric drag (e.g. Passey and Melosh, 1980). Both the elliptical rims and the 'butterfly' ejecta patterns of the craters indicate very shallow impact angles of less than 10° above the horizontal for both impactors (Herrick and Hessen, 2006). All of this information strongly constrains the event that formed the double crater.

The impact kinetic energy available for the excavation of each crater can be estimated from their dimensions, using 'equivalent' crater diameters given by $D = 2(ab)^{1/2}$ (where a and b are the major and minor semi-axes of the crater), and the simple diameter (D) vs impact energy (IE) relation:

$$D = D_0\left(\frac{IE\sin\theta}{IE_0}\right)^{1/3},$$

where IE_0 and D_0 are reference values of IE and D, and θ is the impact angle, referred to the horizontal (see Chappelow and Sharpton, 2005, and references therein). Assuming a conservative value of impact angle of 10°, these energies turn out to be approximately

* Corresponding author at: Geophysical Institute, University of Alaska Fairbanks, PO Box 757320, Fairbanks, AK 99775-7320, USA. Fax: +1 (907) 474 7184.
E-mail address: john.chappelow@gi.alaska.edu (J.E. Chappelow).

0019-1035/$ – see front matter
doi:10.1016/j.icarus.2008.06.001

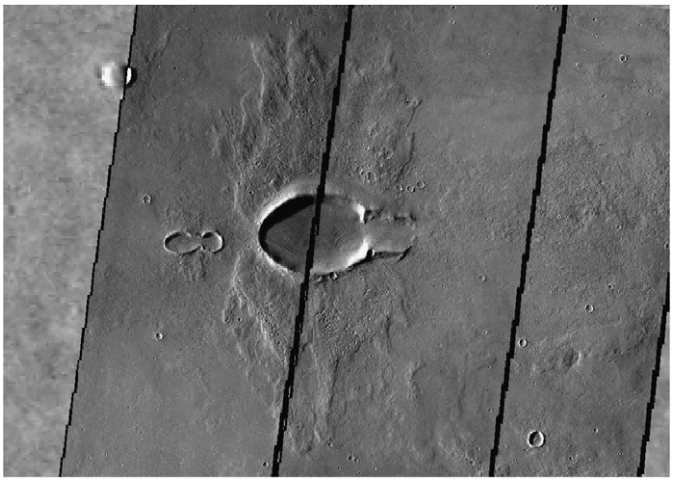

Fig. 1. A large (7.5 × 10.0 km) elliptical crater with a smaller elliptical crater (2.0 × 3.0 km) lying 12.5 km directly uprange (to the left). 'Butterfly'-pattern ejecta occur around both craters. (Mosaic of THEMIS daytime IR images.) North is up.

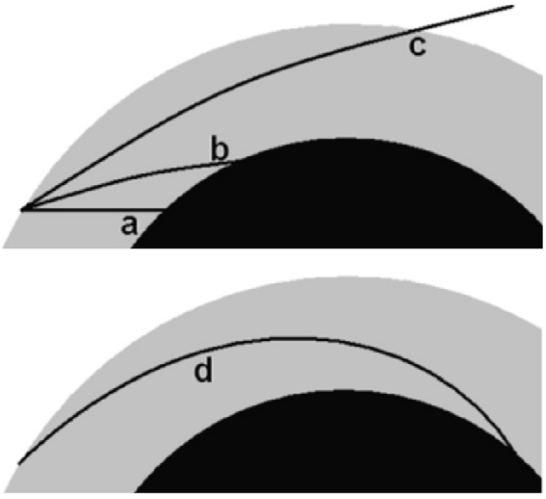

Fig. 2. Atmospheric flight trajectories for asteroids (top) and a moonlet (bottom) in the martian atmosphere, as discussed in the text. Both are radially exaggerated.

3.3×10^{19} and 7.5×10^{17} J for the large and small craters, respectively. These estimates are conservative because they are minimum values; impacts at smaller angles would require higher impact energies, and therefore larger projectiles, to form the same craters.

It is important to note that these 'impact energies' are not the same as the total kinetic energies the impactors have at the moment of contact. Due to Mars's rotation, and the very shallow impact angles involved, the target surface is moving about 180 m s^{-1} in essentially the same direction as the projectiles at time of impact. So not all of their kinetic energies are available to contribute to crater excavation, only that part associated with the velocities of the impactors relative to the (moving) surface. Thus the impact energies (*IE*) will be less than the final kinetic energies (KE_{final}). This subject is discussed more fully below.

2. Possible formation events

Dismissing as extremely unlikely the possibility that the two craters were formed by two independent events, reasonable possibilities for the double crater's provenance include: (1) a single extra-martian asteroid which fractured in the atmosphere and the two fragments were then separated by differential drag deceleration, (2) a single asteroid which was fractured by tidal forces, and the fragments then separated to some degree, before atmospheric entry, (3) the impact of a double asteroid, (4) the impact of an areocentric moonlet which fractured in the atmosphere after its orbit tidally decayed, and its fragments separated under atmospheric drag as in case (1). A final possibility (5) is that an object passed into and back out of Mars's atmosphere, losing enough kinetic energy in the process to enter a highly elliptical, bound orbit about Mars. Repeated passes through Mars's atmosphere would quickly bring such an object down on a trajectory similar to that of case (4) above.

2.1. Case (1)

Case (1) seems at first the most reasonable scenario since the only obvious requirements are an incident asteroid of the right energy to form the craters, a single fracturing event resulting in two fragments, and an atmospheric time-of-flight long enough to allow the fragments to separate by 12.5 km due to drag. However, the average relative velocity of Mars-incident asteroids is ~10.2 km s^{-1} (e.g. Davis, 1993), and their minimum relative velocity is 5.0 km s^{-1} (martian escape velocity at 100 km altitude, defined herein as the top of the martian atmosphere). At these speeds most of them take only a few seconds, up to a few tens of seconds, to pass completely through Mars's atmosphere and strike the surface (path 'a,' Fig. 2). Even for those that encounter Mars at nearly 'surface-grazing' incidence (path 'b,' Fig. 2), the atmospheric flight time is less than about 80 s, for 10.2 km s^{-1} entry velocity. Thus there is little time-of-flight for differential drag to act and, depending upon their masses and densities, and upon the atmospheric density, the drag applied by the atmosphere may have little effect on impactors large enough to form the craters in question, much less the ability to separate a pair of them by 12.5 km. Obviously, asteroids that enter at too-shallow angles will simply pass through the atmosphere (path 'c,' Fig. 2).

To evaluate case (1), an atmospheric entry and passage model was used to try to reproduce the event that formed the craters, including the shallow impact angles, the sizes of the two craters and their relative positions. The model basically consists of a fourth order Runge–Kutta numerical method used to integrate the equations of motion of meteoritic flight through a simple exponential atmosphere (see Chappelow and Sharpton, 2005, 2006). Using this model, pairs of simulated 'test fragments,' each *pair* representing a single, initially unfragmented object, were launched from an altitude of 100 km (~9 martian atmospheric scale heights). Both objects of each pair were given identical entry angles and velocities of 5.0 km s^{-1}. Physical properties were set consistent with carbonaceous chondrite materials (heat of ablation = 3200 kJ kg^{-1}; Chyba et al., 1990), except for the density which was given a relatively low value of 1800 kg m^{-3} (similar to Phobos and Diemos, but less than most asteroids) in order to favor drag separation. All of the calculations were carried out for hypothetical martian atmospheres of 60 and 600 mbar of surface pressure, in addition to Mars current average of 6 mbar.

Assigning initial masses to the test fragments was somewhat more problematic. These values must be set so that the eventual impacts with the surface produce craters of the right sizes, so they must be obtained from the impact energies (*IE*). The idea is to use the *IE* estimates obtained from the crater dimensions to determine the kinetic energy each fragment had at impact (KE_{final}), next use KE_{final} to estimate the kinetic energy at atmospheric entry (KE_{entry}), then use KE_{entry} together with the entry velocity given above to fix each fragment's mass.

KE_{final} can be obtained from *IE* as follows: the target surface moves away from (in roughly the same direction as) an eastbound, low-impact-angle projectile, so the projectile's velocity relative to the target is approximately $v_{\text{rel}} \approx v_{\text{obj}} - v_{\text{targ}}$, where v_{obj} and v_{targ}

Table 1
Results of simulations of asteriod impact on Mars as described in the text

Atmosphere (mbar)	Entry conditions		Impact conditions (big mass/small mass)			Impact separation (km)
	Masses (big mass/small mass) (kg)	Entry angle (°)	Masses (kg)	Velocities (km s^{-1})	Impact angles (°)	
6	2.75e12/6.23e10	10.0	2.75e12/6.23e10	5.07/5.07	2.57/2.58	0.2
6	2.75e12/6.23e10	9.9	2.75e12/6.23e10	5.07/5.06	2.15/2.16	0.3
6	2.75e12/6.23e10	9.8	2.75e12/6.23e10	5.07/5.06	1.62/1.63	0.5
6	2.75e12/6.23e10	9.7	2.75e12/6.23e10	5.07/5.05	0.81/0.83	1.6
6	2.75e12/6.23e10	9.6	MISS			
60	2.79e12/6.54e10	10.0	2.79e12/6.54e10	5.04/4.95	2.59/2.65	1.8
60	2.79e12/6.54e10	9.9	2.79e12/6.54e10	5.03/4.94	2.17/2.24	2.7
60	2.79e12/6.63e10	9.8	2.79e12/6.62e10	5.03/4.92	1.66/1.75	4.6
60	2.79e12/6.71e10	9.7	2.79e12/6.70e10	5.02/4.89	0.89/1.07	12.2
60	2.79e12/6.71e10	9.6	MISS			
600	3.07e12/8.89e10	10.5	3.06e12/8.87e10	4.82/4.31	4.23/4.49	4.8
600	3.16e12/9.47e10	10.0	3.16e12/9.45e10	4.74/4.14	2.78/3.24	13.3
600	3.20e12/9.69e10	9.9	3.19e12/9.66e10	4.72/4.09	2.41/2.94	18.0
600	3.25e12/9.97e10	9.8	3.24e12/9.95e10	4.68/4.02	1.97/2.62	26.1
600	3.32e12/1.03e11	9.7	3.32e12/1.03e11	4.63/3.94	1.42/2.28	43.1
600	3.55e12/1.10e11	9.6	3.54e12/1.10e11	4.48/3.84	0.46/1.88	109.5
600	3.55e12/1.10e11	9.5	MISS			

Rows marked 'MISS' represent objects which failed to hit Mars but escape the atmosphere instead. The entry velocity was 5.0 km s^{-1} and the asteroid density 1800 kg m^{-3} in each case.

Table 2
Results for more realistic Mars-incident asteroidal objects than those presented in Table 1

Atmosphere (mbar)	Entry conditions		Impact conditions (big/small)			Impact separation (km)
	Masses (big/small) (kg)	Entry angle (°)	Masses (kg)	Velocities (km s^{-1})	Impact angles (°)	
6	6.78e11/1.54e10	12.9	6.78e11/1.54e10	10.03/10.00	1.70/1.70	0.08
6	6.78e11/1.54e10	12.8	6.78e11/1.54e10	10.02/9.99	0.51/0.52	0.48
6	6.78e11/1.54e10	12.7	MISS			
60	6.88e11/1.67e10	12.9	6.87e11/1.66e10	9.94/9.71	1.71/1.73	0.81
60	6.88e11/1.67e10	12.8	6.87e11/1.66e10	9.91/9.62	0.55/0.63	4.06
60	6.88e11/1.67e10	12.7	MISS			

The entry velocity is 10 km s^{-1} and the asteroid density is 2500 kg m^{-3}. Rows marked 'MISS' represent objects which failed to hit Mars but would escape the atmosphere instead.

Table 3
Results for a minimum-entry-velocity, surface-grazing, short-period comet

Atmosphere (mbar)	Entry conditions		Impact conditions (big/small)			Impact separation (km)
	Masses (big/small) (kg)	Entry angle (°)	Masses (kg)	Velocities (km s^{-1})	Impact angles (°)	
6	3.49e11/8.29e09	13.3	3.44e11/7.88e09	13.99/13.91	1.34/1.34	0.113
60	4.09e11/1.31e10	13.3	3.58e11/8.94e09	13.71/13.03	1.35/1.39	1.124

are the speeds of the projectile and the target relative to Mars's center. The kinetic energy available to excavate a crater is then:

$$IE = \frac{1}{2}mv_{\mathrm{rel}}^2 = \frac{1}{2}m(v_{\mathrm{obj}} - v_{\mathrm{targ}})^2.$$

The total kinetic energy of m at impact is actually

$$KE_{\mathrm{final}} = \frac{1}{2}mv_{\mathrm{obj}}^2.$$

Thus the fraction of KE available for cratering is

$$\frac{IE}{KE_{\mathrm{final}}} = \frac{1/2m(v_{\mathrm{obj}} - v_{\mathrm{targ}})^2}{1/2mv_{\mathrm{obj}}^2} \approx 1 - 2\frac{v_{\mathrm{targ}}}{v_{\mathrm{obj}}}.$$

For an impactor striking at ~5 km s^{-1} at 40° north latitude, this fraction is 0.93. Thus, for this example, we would have to add ~7% to the impact energy as derived from the crater dimensions to get the actual kinetic energy of the projectile at impact.

Next KE_{entry} must be related to KE_{final}. A simple energy balance equation for the descent of a fragment from entry to impact can be written:

$$KE_{\mathrm{final}} = KE_{\mathrm{entry}} + (PE_{\mathrm{entry}} - PE_{\mathrm{final}}) - E_{\mathrm{drag}}, \quad (1)$$

where KE and PE are kinetic and gravitational potential energies. Note that this equation neglects kinetic energy lost due to mass ablation from the impactors. However, as we shall show, ablation plays a very minor role (see Tables 1, 2 and 4) in all but a certain extreme case (see Table 3). The term $(PE_{\mathrm{entry}} - PE_{\mathrm{impact}})$ is the amount of gravitational potential energy exchanged for kinetic energy, and E_{drag} is the kinetic energy lost to drag dissipation, as a given fragment descends through the atmosphere. It is easy to show that the potential energy 'lost' is a small fraction, f, of KE_{entry}, where:

$$f = \frac{2gz_0}{v_0^2}$$

Table 4
Results of the moonlet cases discussed in the text

Atmosphere (mbar)	Entry conditions		Impact conditions (big/small)			Impact separation (km)
	Masses (big/small) (kg)	Entry angle (°)	Masses (kg)	Velocities (km s^{-1})	Impact angles (°)	
6	5.63e12/1.27e11	0	5.63e12/1.27e11	3.60/3.59	1.37/1.42	11.9
60	5.77e12/1.38e11	0	5.77e12/1.38e11	3.56/3.46	1.53/1.89	81.2

and z_0 and v_0 are the starting values of altitude and speed, and g is the acceleration due to gravity (assumed constant). With a little rearranging Eq. (1) becomes:

$$KE_{\text{final}} = (1 + f)KE_{\text{entry}} - E_{\text{drag}}.$$

Given the starting altitude (100 km), and minimum asteroidal velocity of 5.0 km s^{-1}, f comes to 0.029 for an extra-martian asteroid.

The drag contribution is harder to quantify since it depends on several variables and cannot be handled analytically. For the 6 mbar atmosphere, test runs of the numerical simulation indicate that the drag dissipation term is two to three orders of magnitude smaller than the kinetic energy for all entry angles of interest, and is therefore negligible. However, this does not hold for the denser atmospheres. In those cases, the masses must be determined by iteratively conducting test runs to zero-in on the appropriate values of mass. The requirement used here is that the impact energies calculated from the simulation be approximately the same as those calculated from the crater dimensions (a criterion of ±2% was used). Once the proper masses were determined a final, 'real,' run was executed and the results recorded.

The procedure described above was repeated for multiple entry angles, for each of the atmospheres studied. The results are summarized in Table 1. It is clear that the differential drag applied by the 6 mbar atmosphere simply cannot produce enough separation between the test-impactors to produce two separate craters, much less ones separated by 12.5 km. The 60 mbar atmosphere can, in principle, sufficiently separate the craters, but only if the asteroid enters an "entry corridor" less than 0.2° wide, centered about $\theta = 9.7°$; according to the $\sin^2\theta$ probability distribution, less than 0.1% of asteroids do this. This entry corridor is wider for the 600 mbar atmosphere case, however, as mentioned above, such a dense atmosphere (100's of mbar) is apparently inconsistent with the late Hesperian time-frame of the impact event.

In view of these results, and especially in view of the strong assumptions that were made obtaining them (very low density impactors, lowest possible entry velocity, conservative estimate of impact energy), it appears extremely unlikely that the double crater could have been produced by an extra-martian asteroid, fragmentation and impact event. Program runs conducted using more realistic virtual asteroids (density = 2500 kg m^{-3}, entry velocity = 10.0 km s^{-3}) reinforce this conclusion (Table 2); for these asteroids even the 60 mbar atmosphere is insufficient to separate the impacts by more than a few kilometers.

An alternate possibility is that the craters were formed by a comet rather than an asteroid. With their lower densities (~1000 kg m^{-3}), and heats of ablation ~1600 KJ kg^{-1} (see Chappelow and Sharpton, 2005, and references therein), icy objects may be more effectively slowed by drag than asteroids. However they also arrive at Mars with a minimum entry velocity of about 14 km s^{-1} (e.g. Chappelow and Sharpton, 2005). In addition they are constitutionally weaker, and so possibly subject to catastrophic fragmentation ('airburst') even in thin atmospheres.

To investigate this we set up our program to simulate the entry and impact of a comet with its minimum possible speed, and on a trajectory that just grazes the surface of Mars. Results of runs through 6 and 60 mbar atmospheres show some differences compared to the asteroid cases, but nothing unexpected. Here the fragments are considerably less massive than before due to their higher velocities, though this is compensated for somewhat by ablation which is much more significant, especially for the smaller fragment. Again, the fragments land much too close together to form the double impact crater observed (Table 3), even given every favorable condition, and of course neglecting the possibility of catastrophic disruption in the atmosphere (even though dynamic pressures reach the MPa-range in both cases).

2.2. Cases (2) and (3)

Cases (2) and (3) are identical in most respects that have to do with formation of the double crater in question, and are therefore treated here together. First, consider the impact of a pair of objects, one (m) significantly smaller than the other (M), vertically incident on an airless surface. Defining the impact point of the larger object as a reference point, O, the azimuthal direction of the smaller impact relative to O will be random if the orientation of the original pair of objects with respect to each other was itself random, as is the case for our putative asteroid. If L represents the distance between m and M, perpendicular to their mutual direction of flight, then the location of possible impact points of m forms a circle (S) of radius L about O (Fig. 3a). The probability (P) of m impacting any given segment, δS, of curve S is the length of that segment, normalized by the circumference of S:

$$P = \frac{\int_{\delta S} \mathrm{d}S}{\oint_S \mathrm{d}S}. \tag{2}$$

This also holds true if the two objects impact at a non-vertical angle, θ (measured from the horizontal), though in this case S is an ellipse with semi-minor axis L and semi-major axis $L/\sin\theta$, oriented parallel to the ground track (Fig. 3b). Thus, the effect of an oblique impact angle is to stretch S, and bias P, in the uprange and downrange directions. In addition, if an atmosphere is present differential drag will have the effect of shifting S in the uprange direction (Fig. 4c). However, the results shown in the last column of Table 2 demonstrate that except under extreme circumstances (e.g. entry into a much denser martian atmosphere than today's, and on almost exactly a surface-grazing trajectory) the effect of differential drag on a typical Mars-encountering asteroid of the appropriate size to form the observed craters is negligibly small.

The smaller of the two elliptical craters studied here lies within 3.5° of directly uprange of the larger (Fig. 4). For an impact angle of $\theta = 5°$, Eq. (2) yields a probability of $P = 0.115$, or less than one-chance-in-eight, that m would impact within ±4° of directly uprange of M, purely by chance. For a 10° impact angle the corresponding number is $P = 0.049$, or about one-chance-in-twenty. Thus, if this were a double asteroid impact, we should expect to see others where the two craters are not aligned as they are here (for example, side-by-side, or with the smaller crater downrange of the larger) yet we do not see this.

The above probabilities are obviously for doublet impacts, which are themselves relatively rare events. Bottke and Melosh (1996) estimated that only about ~2% of martian craters in this

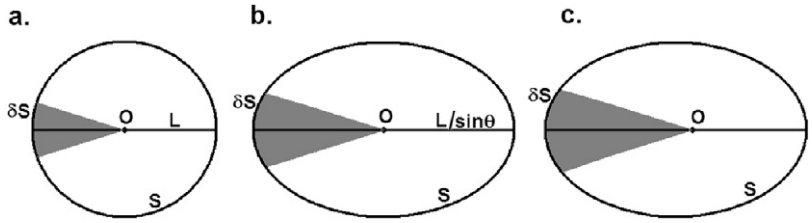

Fig. 3. Geometry of relative positioning of impacting objects which are randomly oriented with respect to each other upon atmospheric entry. The larger object impacts at O, the smaller somewhere on arc δS. (a) Vertical incidence, no atmosphere. (b) Oblique incidence, no atmosphere. (c) Oblique incidence, with atmosphere; the length of δS increases because point O is shifted to the right.

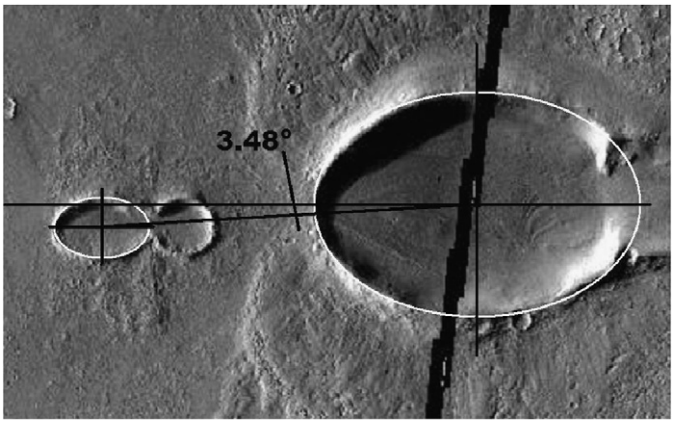

Fig. 4. Measurement of the offset of the small crater from due-uprange of the large crater. The small crater is approximately 3.5° from directly uprange of the larger crater.

size range are doublets. This pair of craters was identified as part of a comprehensive survey of craters in the northern lowlands that found a total of 300 craters on flat terrain with well-preserved ejecta blankets (Herrick and Hessen, 2006). Of those craters, only 9 (3%) were at low enough angle to be elliptical and have butterfly ejecta blankets. The expected percentage (of the 300 identified craters) that would be elliptical, doublet, asteroid impacts with the smaller crater within 4 degrees of uprange is therefore about $2 \times 10 \times 3\%$. So the odds are roughly 1-in-50 that one of the 9 butterfly craters would be a double, oblique impact with the smaller crater directly uprange of the larger, if the source were a double, extra-martian asteroid. Yet one of the 9 is, in fact, just such a crater. Thus, though we cannot rule it out, we consider it unlikely that the feature was formed by a double asteroid.

This same argument applies to the possibility of aerodynamic side-forces (e.g. 'lift') playing a significant role in separating the impactors, since such forces would be randomly directed.

2.3. Case (4)

In case (4) we envision a small martian moon whose orbit has tidally decayed to the point that it encounters the top of Mars's atmosphere (herein defined as 100 km altitude). It enters the atmosphere at an extremely shallow angle and at about 3.5 $\mathrm{km\,s^{-1}}$, which is circular velocity for this altitude. At some point during its descent it fragments into two large pieces, one approximately forty times the mass of the other, under aerodynamic forces. Path 'd' in Fig. 2 illustrates the atmospheric trajectory the putative moonlet, and then both of its fragments, would follow. It must be high enough in the atmosphere when it fragments to allow time for the fragments to separate, but the flight-path length is much longer than for any incident asteroid (paths 'a' and 'b,' Fig. 2).

Table 4 summarizes the results of two simulations of such an event; one using today's martian atmosphere the other assuming one ten times denser. Although the 6 mbar case falls slightly short of the 12.5 km of separation required, it adequately demonstrates that even the current martian atmosphere could have caused the double cratering event, via a moonlet. Approximations in the simulation methods, and short period variations in Mars's atmosphere (e.g. seasonal variations, which can amount to several mbar), could easily account for the slight discrepancy. Clearly the 60 mbar atmosphere can also account for the event, even if the moonlet breaks apart much lower in the atmosphere than 100 km. Thus we conclude that the moonlet scenario can explain the formation of this double crater, even under today's conditions. Indeed the result falls right out of this well-constrained case.

If a moonlet *did* form the craters, then (from Table 4) it would have an initial mass of about 5.83×10^{12} kg and, assuming a density of 1800 $\mathrm{kg\,m^{-3}}$, a diameter of about 1800 m, or about 1600 m if its density were 2500 $\mathrm{kg\,m^{-3}}$. In fact, these represent minimum values; the blowouts at the east ends of the craters (Fig. 1), and the extremely shallow predicted impact angles (Table 4) suggest that significant fractions of the projectiles may have 'ricocheted' upon impact, carrying their impact energies downrange with them. If this is the case, the moonlet would have had to be larger to still make the same size craters.

2.4. Case 5

An object entering Mars's atmosphere and re-emerging (as in path 'c,' Fig. 2) would have its velocity reduced in passage and could conceivably emerge with less than escape velocity. It would then go into an "orbit" which would intersect the atmosphere, and make repeated passes until its orbit eventually decayed into an atmospheric trajectory similar to that of the doomed moonlet described above (path 'd,' Fig. 2). If it broke in two during its final entry and descent, the fragments might land close enough to form the double crater.

But all of this depends upon the atmosphere 'aerobraking' the asteroid sufficiently during its first pass-through to drop its speed from greater than v_{esc}, to less than this figure. The problem is, Mars's atmosphere (even a dense one) is only capable of reducing such a large object's velocity by a small amount during this first pass. So the object must have a velocity very close to v_{esc} (perhaps nearly co-orbital with Mars), and must have just the right entry angle, for this to occur.

To demonstrate this we set up the "MISS" cases shown in Table 1 as follows. Leaving the density at 1800 $\mathrm{kg\,m^{-3}}$, the impactor is kept whole, instead of starting as two fragments, and shot into the atmosphere as before ($v_{\mathrm{entry}} = 5$ $\mathrm{km\,s^{-1}}$, $\theta_{\mathrm{entry}} = 9.6°$ or 9.5°). In this case, integration was suspended when the object regained its starting altitude, and its exit velocity was compared to its entry velocity. The results are shown in Table 5.

Only the 600 mbar atmosphere slows its asteroid significantly, even though they all still have unrealistically low densities and entry speeds. And as already stated, such a dense atmosphere seems unlikely to have obtained during the late Hesperian or later. Furthermore, this sort of object would have to fragment only upon its

Table 5
Aerodynamic changes in speed for "MISS" objects from Table 1, for each atmosphere studied

Atmosphere (mbar)	Entry angle (°)	Entry speed ($m\,s^{-1}$)	Exit speed ($m\,s^{-1}$)	Δv ($m\,s^{-1}$)
6	9.6	5000.0	4986	−14
60	9.6	5000.0	4867	−133
600	9.5	5000.0	3805	−1195

final entry into the atmosphere, not during previous passes, or the fragments would separate too much to form the observed feature.

We thus we consider case (5) a very low-order probability.

3. A final speculation

Wherever they came from, Phobos' and Deimos' orbits started in, or evolved into, prograde, near-circular, equatorial orbits, and there is no reason to expect our hypothetical moonlet to behave otherwise. The prograde direction of travel of the crater-forming projectiles therefore provides additional support for the moonlet hypothesis. It would also "track" Mars's equator through its precessions and obliquity changes, much as Phobos and Deimos do (Goldreich, 1965). However the pre-impact orbit it would have been in is inclined to Mars's current equator by about 40°. This suggests that the impact may have occurred at a time when Mars's body-equator was tilted relative to the current one by about 40°, and its north and south rotational poles were located somewhere near 49.5° N, 42.5° E (located east of Lyot Crater) and 49.5° S, 222.5° E (in eastern Terra Sirenum), respectively. The 'true polar wander' this implies would have occurred since the late Hesperian.

4. Conclusions

We have shown that it is very difficult to explain the double, elliptical crater under study by invoking the most obvious explanation for it: the impact of an ordinary Mars-incident asteroid or comet. Even given some very improbable assumptions about the impactor (e.g. lowest possible entry velocity, very low density for an asteroid, most favorable entry angle), it appears nearly impossible to reproduce the observed crater separation with an extra-martian asteroid, unless one also assumes an implausibly high atmospheric density. The shallow entry angle, and narrow entry corridor required to get any separation between the fragments at all also argues against an asteroidal source.

The impact of a double asteroid or one that has been tidally fractured also appears an unlikely alternative, given that the apparently non-random relative positioning of the craters indicates that separation of the impactors was probably due to differential drag deceleration, and not random chance. Such an event is also statistically unlikely, though it cannot be ruled out entirely. The final alternative considered, capture of a passing asteroid via an atmospheric passage also seems highly improbable, since it would require that the projectile have exactly the right entry speed and angle in order to be drag-decelerated below escape velocity.

Although it has not been proved that the observed double crater was formed by an impacting moonlet, it has been shown that this theory is a viable alternative. It naturally accounts for all the noted features, particularly the separation distance and relative positions, of the craters even for a martian atmosphere as thin as today's, and without invoking an extraordinary event.

Acknowledgments

The authors wish to thank Dr. Olga Popova and an anonymous reviewer for their thoughtful reviews of this work. J.E.C. also acknowledges Dr. William Bottke for thoughtful insights. This work was supported by a University of Alaska Fairbanks Arctic Region Supercomputing Center post-doctoral appointment to J.E.C.

References

Bottke, W.F., Melosh, H.J., 1996. Binary asteroids and the formation of doublet craters. Icarus 124, 372–391.
Bottke, W.F., Love, S.G., Tytell, D., Glotch, T., 2000. Interpreting the elliptical crater populations on Mars, Venus, and the Moon. Icarus 145, 108–121.
Chappelow, J.E., Sharpton, V.L., 2005. Influences of atmospheric variations on Mars's record of small craters. Icarus 178, 40–55.
Chappelow, J.E., Sharpton, V.L., 2006. Atmospheric variations and meteorite production on Mars. Icarus 184, 424–435.
Chyba, C.F., Thomas, P.J., Brookshaw, L., Sagan, C., 1990. Cometary delivery of organic molecules to the early Earth. Science 249, 366–373.
Craddock, R.A., Howard, A.D., 2002. The case for rainfall on a warm, wet early Mars. J. Geophys. Res. 107 (E11), doi:10:1029/2001JE001505. 5111.
Davis, P.M., 1993. Meteoroid impacts as seismic sources on Mars. Icarus 105, 469–478.
Gault, D.E., Wedekind, J.A., 1978. Experimental studies of oblique impact. Proc. Lunar Sci. Conf. 9, 3843–3875.
Goldreich, P., 1965. Inclination of satellite orbits about an oblate precessing planet. Astron. J. 70, 5–9.
Herrick, R.R., Hessen, K.K., 2006. The planforms of low-angle impact craters in the northern hemisphere of Mars. Meteorit. Planet. Sci. 41, 1483–1495.
Jakosky, B.M., Phillips, R.J., 2001. Mars' volatile and climate history. Nature 412, 237–244.
Lambeck, K., 1979. On the orbital evolution of martian satellites. J. Geophys. Res. 84, 5651–5658.
Passey, Q.R., Melosh, H.J., 1980. Effects of atmospheric breakup on crater field formation. Icarus 42, 211–233.
Schultz, P.H., Lutz-Garihan, A.B., 1982. Grazing impacts on Mars: A record of lost satellites. J. Geophys. Res. 87 (Suppl.), A84–A96.
Tanaka, K.L., Skinner, J.A., Hare, T.M., 2005. Geologic map of the northern plains of Mars. US Geol. Surv. Sci. Invest. Map, SIM 2888.